Modeling of the gas-phase chemistry in C–H–O gas mixtures for diamond chemical vapor deposition

James R. Petherbridge, Paul W. May,[a] and Michael N. R. Ashfold
School of Chemistry, University of Bristol, Bristol, BS8 1TS United Kingdom

(Received 21 November 2000; accepted for publication 8 February 2001)

The boundaries of the diamond deposition region in the C–H–O (Bachmann) atomic phase composition diagram have been reproduced successfully for 38 different C, H, and O containing gas mixtures using the CHEMKIN computer package, together with just two criteria—a minimum mole fraction of methyl radicals [CH_3] and a limiting value of the [H]/[C_2H_2] ratio. The diamond growth/no-growth boundary coincides with the line along which the input mole fractions of C and O are equal. For every gas mixture studied, no-growth regions are found to coincide with a negligible ($<10^{-10}$) mole fraction of CH_3 radicals, while for gas mixtures lying within the diamond growth region the CH_3 mole fraction is $\sim 10^{-7}$. Each no-growth→diamond growth boundary is seen to be accompanied by a 2–3 order of magnitude step in CH_3 mole fraction. The boundary between diamond and nondiamond growth is less clearly defined, but can be reproduced by assuming a critical, temperature dependent [H]/[C_2H_2] ratio (0.2, in the case that $T_{gas}=2000$ K) that reflects the crucial role of H atoms in the etching of nondiamond phases. The analysis allows prediction of the composition process window for good quality diamond growth for all stable input gas mixtures considered in this study. © *2001 American Institute of Physics.*
[DOI: 10.1063/1.1360221]

I. INTRODUCTION

Low-pressure diamond deposition has been achieved using a large range of C, H, and O containing gas mixtures. Bachmann *et al.*[1,2] summarized the results of many deposition experiments involving various gas mixtures and reactor types in the form of an atomic C–H–O phase diagram. They concluded that the exact nature of the source gases was unimportant for most diamond chemical vapor deposition (CVD) processes and that, at typical process temperatures and pressures, it was only the relative ratios of C, H, and O that controlled deposition. The diagram partitions into three distinct regions associated with: (a) diamond growth, centered on the C–O tie line where the input mole fractions of carbon and oxygen are equal (i.e., [C]=[O]); (b) no growth, lying below the C–O tie line (i.e., [C]<[O]); and (c) nondiamond growth, located above the C–O tie line (i.e., [C] >[O]). Experiments by Marinelli *et al.*,[3] using a variety of hydrocarbon/CO_2 gas mixtures, confirmed the presence of three such regions, and also refined the position of the boundaries between them. Beckmann *et al.*[4] investigated a limited number of cuts across the C–O tie line, using a model that considered just gas phase reactions, and concluded that oxygen regulated the concentration of reactive carbon species by reaction to form CO, thus accounting for the no-growth region for [C]<[O]. Ford[5] modeled the competition between diamond and nondiamond growth, and found the boundary between these two regions to correlate with the line ([C]–[H])/[O])=0.07 in the Bachmann diagram. More recently, Eaton and Sunkara[6] used a CHEMKIN model that considered both gas phase and gas-surface chemistry to calculate mole fractions of C, H, and O containing radical species, which were then plotted in the form of a ternary C–H–O diagram. We note, however, that this study covers only a small section of the conventional Bachmann diagram. Here we present CHEMKIN simulations of gas mixtures corresponding to 38 cuts through large widely spaced portions of the Bachmann diagram, which allow prediction of the boundaries of the whole diamond deposition domain and of the respective process windows for successful diamond growth for the various stable gas mixtures considered.

II. SIMULATIONS

The gas phase reactions occurring in a representative gas phase environment used for diamond CVD were simulated using the SENKIN code, which is part of the CHEMKIN package.[7] All of the C, H, and/or O containing species reactions and temperature dependent rate constants used in these calculations were obtained from the GRI-Mech 2.11 reaction mechanism.[8] In the case of CO_2/CH_4 mixtures, the following reactions have been identified[9] as being of particular importance:

$$CO_2+CH_4 \leftrightharpoons 2CO+2H_2, \quad (1)$$

$$2CH_4 \leftrightharpoons C_2H_2+3H_2, \quad (2)$$

$$CO_2+H_2 \leftrightharpoons CO+H_2O, \quad (3)$$

$$H_2O+C_2H_2 \leftrightharpoons CH_4+CO. \quad (4)$$

Though, in each case it should be recognized that each of these overall transformations appears in the mechanism as a series of elementary reactions. The GRI-Mech 2.11 database

[a]Author to whom correspondence should be addressed; electronic mail: paul.may@bris.ac.uk

contains over 200 reactions involving C, H, and/or O containing species, all of which were included in the simulations. Equilibrium mole fractions of the 29 transient and stable gas phase species involved in this reaction scheme were calculated, for many different input gas mixtures (e.g., 50% CO_2/50% CH_4), at a fixed gas temperature, T_{gas}, (e.g., 2000 K) and pressure (40 Torr). Obvious limitations inherent in this approach include the following.

(1) The assumption of a single temperature (e.g., 2000 K) for all reactions. 2000 K is considered to be representative of the gas temperature within the plasma in low power (<3 kW) microwave (MW) CVD chambers at ~40 Torr.[10] This temperature has been used successfully to model species mole fractions in a CO_2/CH_4 microwave plasma,[9] and is comparable to that prevailing in the immediate vicinity of the filament in hot filament CVD. However, it should be noted that in MW reactors which operate at higher powers (>5 kW) and increased pressures (several hundred Torr) the gas phase chemistry can be rather different, thus altering the positions of the various growth/non-growth regions of the Bachmann diagram. Since data for the process windows in these higher power processes are still scarce in the literature, we limit ourselves in this work to the more conventional lower power systems for which the standard Bachmann diagram is valid.

(2) No electron impact dissociation, ionic reactions, or surface chemistry are included in the modeling. Reaction is thus initiated solely by thermal dissociation.

(3) No transport into or out of the reaction volume is considered. To mimic experiment, therefore, it is necessary to run the simulation for a finite (user selected) time, *t*. The calculations reported here employ $t=5$ s, but the calculated species mole fractions were found to be insensitive to the choice of simulation time in the range $1 \leqslant t \leqslant 300$ s, reflecting the speed with which equilibrium is attained.

III. RESULTS AND DISCUSSION

Calculations were carried out for 38 gas mixtures, exploring the full composition range in each case (e.g., 100% CH_4 to 100% H_2 for a CH_4/H_2 mixture). All combinations of each of the hydrocarbons CH_4, C_2H_2, C_2H_3, C_2H_4, C_2H_5, and C_2H_6, with each of the species CO, CO_2, O_2, H_2O, OH, and HO_2 were considered, as well as CH_4/H_2 and C_2H_2/H_2 mixtures. Figure 1 shows the calculated variation in the mole fractions of H atoms, CH_3 radicals, and H_2, C_2H_2, and CO molecules over the full composition range for four representative gas mixtures: (a) CO_2/H_2O, (b) CO_2/CH_4, (c) CH_4/H_2, and (d) CO/C_2H_4, at $T_{gas}=2000$ K. These four gas mixtures are also shown as lines (a)–(d) crossing a Bachmann diagram in Fig. 2. The calculated compositions are considered in turn, first from the perspective of the CH_3 radical which is generally considered to be the primary growth species in most low pressure diamond CVD environments.[9,11,12]

Figure 1(a) illustrates that the CO_2/H_2O gas mixture is comparatively unreactive; the CH_3 mole fraction (denoted as $[CH_3]$) is negligible ($<10^{-10}$) for all compositions and, consequently, no production of C_2H_2 (the most stable product from CH_3 radical recombination) is seen. The chemistry prevailing in CO_2/CH_4 gas mixtures [Fig. 1(b)] has been discussed in some detail elsewhere.[9] We find $[H_2]$, [CO], and [H] are relatively high over the entire range of compositions, but $[CH_3]$ is $<10^{-10}$ at all compositions below 50% CH_4 (i.e., >50% CO_2). As soon as the $[CH_4]/[CO_2]$ input gas ratio exceeds unity, $[CH_3]$ is predicted to rise sharply (to $>10^{-6}$) and the C_2H_2 mole fraction grows rapidly. For the CH_4/H_2 gas mixture [Fig. 1(c)] the $[CH_3]>10^{-6}$ over the entire composition range, as it is for the CO/C_2H_4 gas mixture after addition of just a few percent of ethene [Fig. 1(d)]. In both cases, $[C_2H_2]$ rises rapidly with increasing hydrocar-

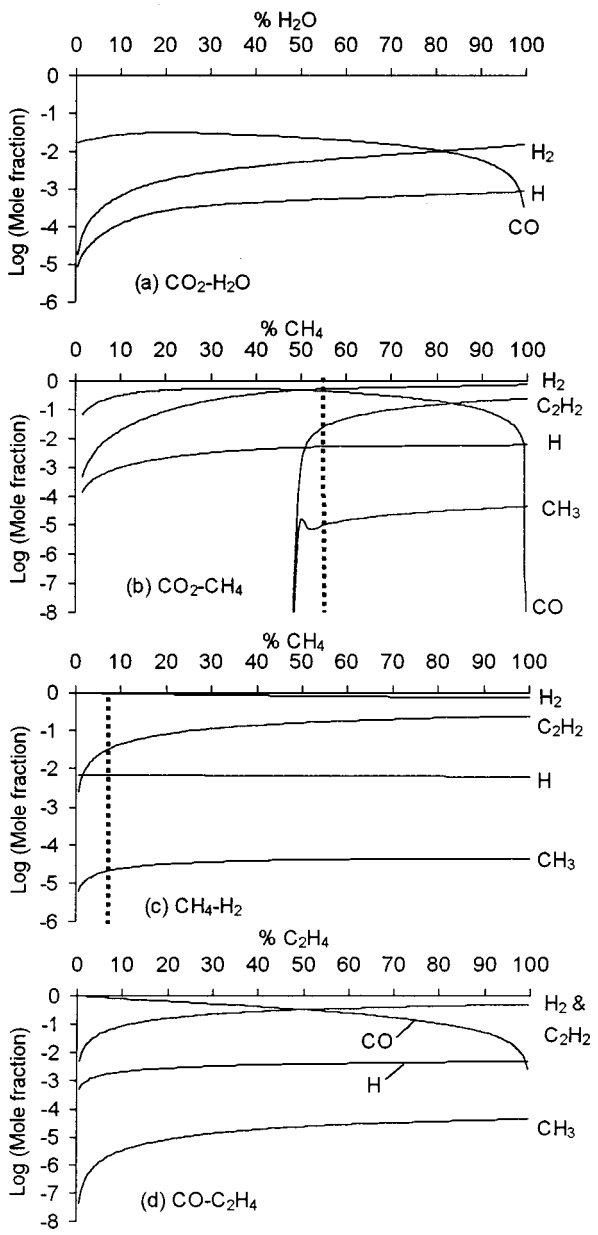

FIG. 1. Calculated species mole fractions for $T_{gas}=2000$ K over the full range of mixing ratios for four different gas mixtures: (a) CO_2/H_2O; (b) CO_2/CH_4; (c) CH_4/H_2; and (d) CO/C_2H_4. The composition for which $[H]/[C_2H_2]=0.2$ is denoted by a vertical dotted line in (b) and (c). Note that $[H]/[C_2H_2] \gg 0.2$ over the entire composition range of the CO_2/H_2O gas mixture, while for CO/C_2H_4 mixtures $[H]/[C_2H_2]<0.2$ over the entire composition range.

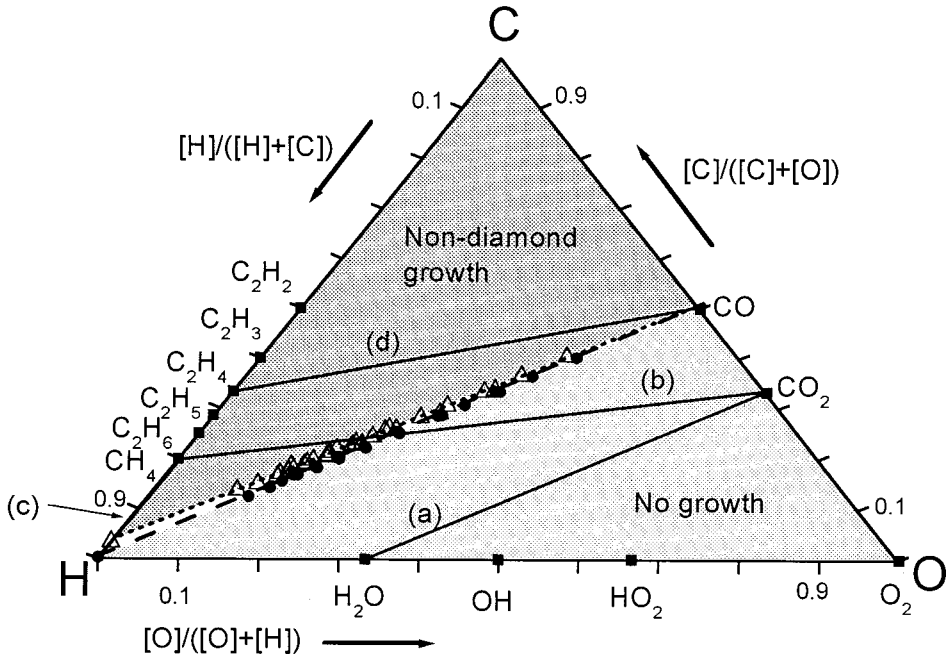

FIG. 2. C–H–O phase diagram for diamond CVD. Gas mixtures investigated in this work lie along the tie lines linking CO, CO_2, O_2, and each H_xO_y species with each hydrocarbon moiety (each represented by a ■ symbol), and along the C–H axis for the case of the CH_4/H_2 and C_2H_2/H_2 gas mixtures. The full lines cutting across the diagram correspond to the four gas mixtures (a) CO_2/H_2O, (b) CO_2/CH_4, (c) CH_4/H_2, and (d) CO/C_2H_4 illustrated in Fig. 1. The dashed (— — —) and dotted (· · · ·) lines indicate the C–O tie line (which forms the boundary between the no-growth and diamond growth regions), and the boundary between diamond and nondiamond growth regions, respectively. Key: ● = composition where, for any given gas mixture, the CH_3 mole fraction increases from $\sim 10^{-10}$ to $\sim 10^{-6}$, △ = composition for which $[H]/[C_2H_2] = 0.2$ at $T_{gas} = 2000$ K.

bon. Figure 2 shows that for these four mixtures, and for all the other gas mixtures studied, the input gas compositions at which $[CH_3]$ jumps up to values $\sim 10^{-7}$ lie along the C–O tie line. Gas mixtures giving $[CH_3] < 10^{-7}$ lie in the no-growth region below the C–O tie line [e.g., the CO_2/H_2O gas mixture shown as line (a)] while all points representing gas mixtures yielding $[CH_3] < 10^{-7}$ fall above the C–O tie line. The existence of the no-growth region in regions where $[C]/[O] < 1$ is thus readily explained by the low CH_3 radical densities in gas mixtures that fall within this part of the Bachmann diagram. A similar step of ~6 orders of magnitude was observed in C_2H_2 concentration, as seen in Figs. 1(b), 1(c), and 1(d). This correlation is due to the rapid recombination of CH_3 radicals[13] leading to the formation of C_2H_2. However, we prefer to define the lower boundary of the diamond domain in terms of $[CH_3]$ because methyl is generally considered to be a diamond growth precursor,[9] whereas C_2H_2 is linked to the deposition of graphite.[14] These calculations also serve to reinforce the suggestion of Beckmann *et al.*[4] that oxygen controls the concentration of reactive carbon species present in the gas phase. Reaction of oxygen and hydrocarbons results in the relatively high concentrations of both CO and H_2 seen in Figs. 1(a) and 1(c).[15] Significant CH_3 concentrations are only produced and build up in gas mixtures lying above the C–O tie line, where $[C] > [O]$. The C–O tie line is therefore the lower boundary of the diamond deposition domain.

The upper boundary of the diamond domain separates the diamond growth and nondiamond growth regions. The distinction between these two regions is less easy to define, and the corresponding boundary is thus less sharp. Here we have assumed that, in order to obtain good quality diamond growth, H atoms must be present at concentrations that are high enough to enable etching of nondiamond phases (often associated with deposition of unsaturated hydrocarbons), and therefore that the boundary between diamond and nondiamond growth must fall at compositions where the ratio of atomic H to unsaturated hydrocarbons exceeds some critical value. Since C_2H_2 is the most abundant unsaturated hydrocarbon arising in the simulations, we investigated the ratio $[H]/[C_2H_2]$ at $T_{gas} = 2000$ K for all 38 gas mixtures and all mixing ratios. We have already shown that $[CH_3]$ is negligible ($< 10^{-10}$) throughout the entire composition range of the CO_2/H_2O gas mixture [Fig. 1(a)]; C_2H_2 is therefore not formed, and the $[H]/[C_2H_2]$ ratio is much greater than unity. For CO_2/CH_4 gas mixtures [Fig. 1(b)], the $[H]/[C_2H_2]$ ratio is similarly large for small CH_4 additions, but declines rapidly once the input mole fraction of CH_4 exceeds 50%, reaching a value of 0.2 when the CH_4/CO_2 mixing ratio is 55/45 and $T_{gas} = 2000$ K. This is the input gas ratio which, experimentally, we judged to represent the boundary separating diamond from nondiamond growth.[9,10]

This encouraged us to explore at what input compositions other gas mixtures yielded $[H]/[C_2H_2]$ ratios of 0.2. In the case of CH_4/H_2 mixtures [Fig. 1(c)], $[H]/[C_2H_2]$ declines with increasing CH_4 additions and passes through the value 0.2 at ~7% added CH_4, while for the CO/C_2H_4 mixture [Fig. 1(d)] the $[H]/[C_2H_2]$ ratio never attains a value of 0.2. The open triangles in Fig. 2 indicate the full range of gas mixing ratios for which $[H]/[C_2H_2] = 0.2$. Very clearly, they lie along a straight line which matches well with the diamond/nondiamond growth boundary deduced from the experimental observations of Marinelli *et al.*[3] Gas compositions below this line give $[H]/[C_2H_2] > 0.2$ while those above it give $[H]/[C_2H_2] < 0.2$. Gas mixtures lying above both the C–O tie line and the $[H]/[C_2H_2] = 0.2$ line fall within the nondiamond growth region [e.g., the CO/C_2H_4 gas mixture shown as line (d)], while mixtures like CO_2/CH_4 which cut through both boundary lines on the Bachmann diagram can support compositions which lie in the no-growth ($[CH_3] < 10^{-7}$), nondiamond growth ($[H]/[C_2H_2] < 0.2$), and diamond growth ($[CH_3] > 10^{-7}$ and

TABLE I. The position of the no-growth/diamond growth and diamond/nondiamond growth boundaries are predicted for a range of gas mixtures in terms of percent hydrocarbon (e.g., $\%C_2H_2$ for C_2H_2/CO_2). These boundaries are compared with the results of some of the available deposition experiments. Simulation conditions: temperature 2000 K, pressure 40 Torr, simulation length 5 s.

	% hydrocarbon			
	No-growth/diamond growth boundary		Diamond/nondiamond growth boundary	
Mixture	Calculated	Experiment	Calculated	Experiment
C_2H_2/CO_2	33.5	(32.0–32.7)[a]	35.0	(32.7–33.4)[a]
C_2H_4/CO_2	33.5	(32.1–35.1),[a] 33[b]	36.1	(35.1–37.1),[a] 35[b]
C_2H_6/CO_2	33.5	(32.5–34.2)[a]	37.0	(34.2–39.4)[a]
CH_4/CO_2	50.0	(47.7–49.1),[a] 50[b]	55.0	(49.1–56.3),[a] 52[b]
C_2H_2/H_2O	33.5		36.3	
C_2H_4/H_2O	33.5		37.1	
C_2H_6/H_2O	33.5		37.0	
CH_4/H_2O	50.0		56.1	
C_2H_2/O_2	50.0		51.5	
C_2H_4/O_2	50.0		52.5	
C_2H_6/O_2	50.0		53.4	
CH_4/O_2	66.5		70.5	
CH_4/H_2	0		7.4	(3–4)[c]

[a]See Ref. 3.
[b]See Ref. 16.
[c]See Ref. 1, and references therein.

$[H]/[C_2H_2] > 0.2$) regions. As Table 1 shows, such analysis allows prediction of the composition process window for good quality diamond growth for all of the various stable input gas mixtures in this study. Agreement with experimental observation is generally very good, except for the case of CO_2/C_2H_2, where theory predicts that both the no-growth/diamond and diamond/nondiamond growth boundaries occur at slightly lower C_2H_2 mixing ratios than experiment,[3] and for the case of CH_4/H_2 gas mixtures, where the $[H]/[C_2H_2] = 0.2$ criterion admits CH_4 mole fractions higher than the ~3% upper limit generally found for reasonable quality diamond deposition.[1]

Two final points merit comment. First, the particular value of the $[H]/[C_2H_2]$ ratio used as the criterion for separating the diamond and nondiamond growth regions is, of course, arbitrary, and also temperature dependent. However, as Fig. 3 illustrates, all of the various input gas compositions identified as lying on this boundary exhibit precisely the same temperature dependent $[H]/[C_2H_2]$ ratio at $T_{gas} \geqslant 1900$ K—emphasizing, once again, the very similar gas phase environment established upon activation of the various gas mixtures used for diamond CVD—and show only minor divergence at lower gas temperatures. Such plots also allow further illustration of the way in which just a small change in mixing ratio can dramatically effect the $[H]/[C_2H_2]$ ratio and, thus, the resulting film composition. For the specific case of CO_2/CH_4 gas mixtures, we identify a 45:55 mixing ratio as the composition corresponding to the diamond/nondiamond growth boundary. Adjusting the input gas mixing ratio to 48:52 leads to a doubling of the calculated $[H]/[C_2H_2]$ ratio at all temperatures, and moves the process well into the diamond growth region of the Bachmann diagram. Conversely, a similarly small compositional shift in the other direction—to a 43:57 mixing ratio—leads to a halving of the calculated $[H]/[C_2H_2]$ ratio, and nondiamond growth. Second, however, we note that the present simulations predict the diamond→nondiamond growth boundary for CH_4/H_2 gas mixtures to lie at 7% CH_4, more than twice the value found experimentally.[1] This may suggest that the criteria governing the boundary between the diamond and nondiamond growth regions may be slightly different for mixtures containing little (or no) oxygen; inspection of Fig. 2 suggests that further experimental study of diamond growth from CH_4/H_2O—as a function of the mixing ratio—could be helpful in this regard. The fact that a simple model that merely allows a gas mixture to react at a given temperature, pressure, and for a set time, has been used to model successfully the boundaries of the Bachmann, diagram indicates that whatever the type of CVD process used (for the conditions investigated) the activation of the gas mixture is the dominant process occurring.

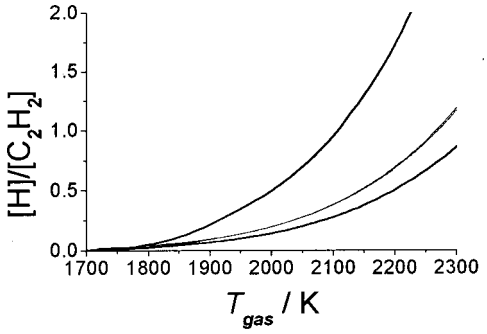

FIG. 3. Plot showing the temperature dependence of the $[H]/[C_2H_2]$ ratio for six different input gas mixtures. The central curve is actually four superimposed curves for the gas mixtures: $55\%CH_4/45\%CO_2$; $7\%CH_4/93\%H_2$; $51\%C_2H_4/49\%CO_2$; $36\%C_2H_2/64\%CO_2$, each of which is identified as lying on the diamond/nondiamond growth boundary. The curves at higher and lower $[H]/[C_2H_2]$ values (for gas mixtures $52\%CH_4/45\%CO_2$ and $57\%CH_4/45\%CO_2$, respectively) illustrate the sensitivity of this ratio to just small changes in the CH_4/CO_2 mixing ratio.

IV. CONCLUSIONS

The three regions (no growth, diamond growth, and nondiamond growth) of the Bachmann diagram have been explored further, via simulation of 38 different input gas mixtures using the CHEMKIN computer package and an assumed gas temperature of 2000 K. The no-growth region is shown to correspond to gas mixtures producing extremely low ($<10^{-10}$) CH_3 mole fractions. Diamond growth is only possible for C, H, and O gas mixtures which yield both sufficiently high ($\sim 10^{-6}$) CH_3 mole fractions to enable deposition of diamond and a H atom mole fraction (defined relative to that of C_2H_2) that is sufficient to etch the nondiamond phases. The nondiamond growth region at $T_{gas} = 2000$ K is found to span gas mixtures where $[CH_3] > 10^{-7}$ but $[H]/[C_2H_2] < 0.2$, under which conditions deposition is presumed to outpace the etching of nondiamond phases.

ACKNOWLEDGMENTS

The authors are grateful to the EPSRC for project funding and De Beers Industrial Diamond Ltd for financial support (J.R.P.), and to Dr. C. M. Western for assistance with implementing the CHEMKIN code.

[1] P. K. Bachmann, D. Leers, and H. Lydtin, Diamond Relat. Mater. **1**, 1 (1991).
[2] P. K. Bachmann, H. J. Hagemann, H. Lade, D. Leers, F. Picht, and D. U. Wiechert, Mater. Res. Soc. Symp. Proc. **339**, 267 (1994).
[3] M. Marinelli, E. Milani, M. Montuori, A. Paoletti, A. Tebano, and G. Balestrino, J. Appl. Phys. **76**, 5702 (1994).
[4] R. Beckmann, B. Sobisch, and W. Kulisch, Diamond Relat. Mater. **4**, 256 (1995).
[5] I. J. Ford, J. Phys. D **29**, 2229 (1996).
[6] S. C. Eaton and M. K. Sunkara, Diamond Relat. Mater. **9**, 1320 (2000).
[7] R. J. Kee, F. M. Rupley, and J. A. Miller, Sandia National Laboratories Report SAND89-8009B (1989).
[8] Gas Research Institute, Chicago, Illinois, Report GRI-97/0020 (1997).
[9] J. R. Petherbridge, P. W. May, S. R. J. Pearce, K. N. Rosser, and M. N. R. Ashfold, J. Appl. Phys. **89**, 1484 (2001).
[10] M. A. Elliott, P. W. May, J. Petherbridge, S. M. Leeds, M. N. R. Ashfold, and W. N. Wang, Diamond Relat. Mater. **9**, 311 (2000).
[11] B. J. Garrison, E. J. Dawnkaski, D. Srivastava, and D. W. Brenner, Science **255**, 835 (1992).
[12] S. J. Harris and D. G. Goodwin, J. Phys. Chem. **97**, 23 (1993).
[13] S. M. Leeds, P. W. May, E. Bartlett, M. N. R. Ashfold, and K. N. Rosser, Diamond Relat. Mater. **8**, 1377 (1999).
[14] S. S. Lee, D. W. Minsek, D. J. Vestyck, and P. Chen, Science **263**, 1596 (1994).
[15] D. G. Goodwin and J. E. Butler, in *Handbook of Industrial Diamonds and Diamond Films*, edited by M. A. Prelas, G. Popovici and L. K. Bigelow (Marcel Dekker, New York, 1998), p. 541, and references therein.
[16] T. P. Mollart and K. L. Lewis, Diamond Relat. Mater. **8**, 236 (1999).